J. Synchrotron Rad. (1996). **3**, 220–224

High-Pressure Cell for the Study of *In-Situ* Hydrates Using Energy-Dispersive X-ray Diffraction

C. C. Tang,[a] C. A. Koh,[b] A. A. Neild,[a] R. J. Cernik,[a] R. E. Motie,[b] R. I. Nooney[b] and J. L. Savidge[c]

[a]CCLRC Daresbury Laboratory, Warrington WA4 4AD, UK, [b]Chemistry Department, King's College London, Strand, London WC2R 2LS, UK, and [c]Gas Research Institute, Basic Research Group, Chicago, Illinois 60631, USA

(*Received 11 April 1996; accepted 5 May 1996*)

A high-pressure low-temperature cell has been developed for *in-situ* diffraction studies of carbon dioxide and propane gas hydrate crystallization. The design and implementation of the cell, which can operate up to 3.5 MPa and down to 253 K, are described. Using synchrotron energy-dispersive X-ray diffraction, the first growth of the hydrate crystals from solution has been successfully observed. The lattice parameters of the hydrate crystals were found to be 11.927 (2) and 17.196 (2) Å, respectively.

Keywords: high-pressure cell; *in-situ* clathration; energy-dispersive powder diffraction.

1. Introduction

The properties of clathrate hydrates have been studied for many years. Extensive reviews and references are given by Davidson (1973), Sloan (1992) and Savidge, Koh, Motie, Nooney & Wu (1996). Our structural understanding of gas hydrates has been based on diffraction studies of samples under static conditions using conventional low-temperature methods (Jeffrey & McMullan, 1967; Jeffrey, 1984). Recently, detailed structural work on argon clathrate has been performed *in situ* by Kuhs, Dorwarth, Londono & Finney (1992) using neutron diffraction. As an alternative development, we have devised a novel *in-situ* technique to probe the sample during crystallization using synchrotron X-rays. This type of work has not been possible before because the availability of photon flux from a laboratory X-ray set is rather limited.

Hydrate crystallization takes place when natural gas and water come into contact at low temperature (~273 K) under high pressure. Under these conditions, polyhedra of hydrogen-bonded water molecules are formed which contain cavities that are able to trap gas molecules. The overall molecular framework normally conforms to one of the two crystal structures described as follows. Structure I has a primitive cubic cell with a lattice parameter of *ca* 12 Å and space group *Pm3n*. In structure II, the space group is *Fd3m*, with a face-centred cubic cell of *ca* 17.2 Å. The CO_2 and C_3H_8 systems are expected to adopt structures I and II, respectively. These two gases were chosen as our 'test' experiments because of their relatively low crystallization pressures, 3.29 and 0.42 MPa, respectively.

The crystallization cell was designed to withstand pressures greater than 3.5 MPa over the temperature range 253–293 K. This cell was then used to synthesize hydrate materials *in-situ* in solution. The cell design also had to take advantage of the unique features of synchrotron radiation: the polychromatic nature of the beam (10–100 keV) and high X-ray flux. For the kinetic studies, it was ideal to collect the whole diffraction pattern simultaneously so that all structural peaks were measured at the same reaction state. The technique of energy-dispersive powder diffraction (EDPD) was therefore well suited to this kind of work (Clark, 1989; He, Barnes, Munn, Turrillas & Klinowski, 1992). The design of the cell and the EDPD instrument are described in subsequent sections.

2. High-pressure cell and sample preparation

The high-pressure cell is shown schematically in Fig. 1. The cell dimensions are approximately 2.5 cm in diameter and 9 cm in height, and the cell was made of austenitic stainless steel (304L). The crucial dimension was the cell-wall thickness as its absorption affects the strength of the diffracted signals. The wall needed to be thin enough to allow maximum X-ray transmission but thick enough for the cell to safely contain the maximum specified pressure. The compromise thickness was calculated and machined down to 0.7 mm over a 32 mm height range to allow access of the beam. The transmission characteristic shown in Fig. 2 was measured on the EDPD instrument (see §3). Using an X-ray beam of 1 mm diameter, the transmitted intensity was obtained from diffraction of a very thin silicon powder (0.1 mm thick) placed inside the cell. The intensity of the (111) reflection was measured as a function of energy. The combination of the dominant absorption effect from the cell wall and the intrinsic intensity-energy spectrum of the instrument, meant that the useful energy range was approximately 30–90 keV and peaked at *ca* 50 keV (see Fig. 2).

The sample chamber (45 ml capacity) was screwed onto a cap fitted with a teflon gasket. The cap was in turn con-

nected to a manifold fitted with a bursting disc (emergency pressure release) rated to 4.0 MPa, a Parr Instruments pressure transducer, gas in and out valves, and a water reservoir. The manifold was also fitted with a depressurizing valve and a vacuum linkage for sample extraction purposes. The vessel was placed in the bored-out Cu block which has gantries cut through to allow the passage of circulating antifreeze/water solution. Sample cooling was controlled by a bath (Grant Ltd) and its temperature was monitored with a thermocouple. The sample temperature was recorded by another sensor which was placed inside the cell. The circulating system was well lagged to improve thermal stability.

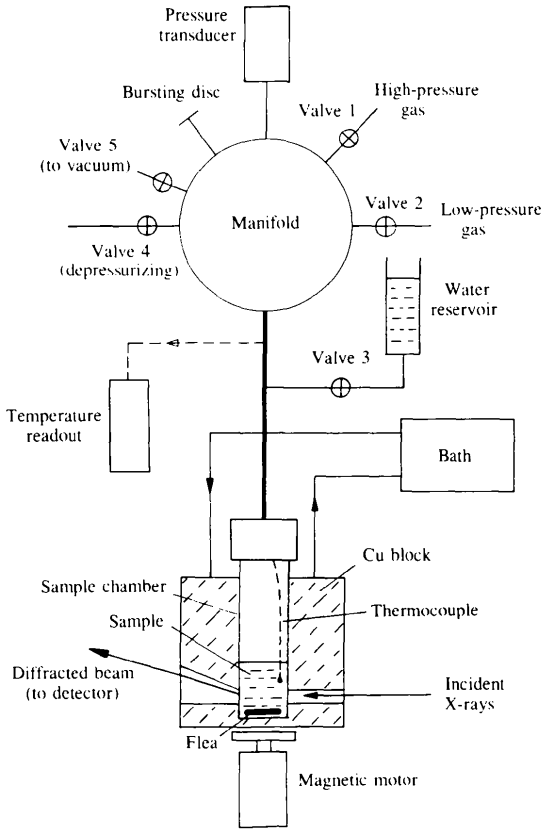

Figure 1
Schematic representation of the gas hydration cell. Hydrate crystals formed in the sample chamber diffract X-rays to the detector.

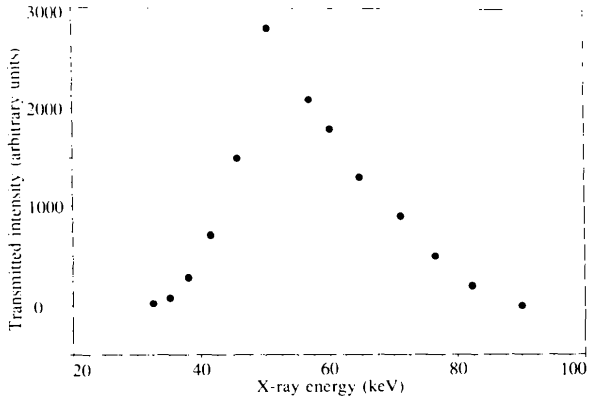

Figure 2
X-ray transmission of the cell measured on the energy-dispersive instrument (station 9.7). The general shape of the curve is essentially the intensity–energy spectrum of the instrument incident onto the cell.

Slots were cut into the front and back of the block for both incident and exit X-ray beams. The block–vessel assembly was then mounted on a stand with vertical and horizontal adjustments so that the slots could be positioned to let the X-ray beams through. The stand housed a magnetic motor to stir the sample in the chamber. The assembled cell was pressure tested off-line up to 5.6 MPa before it was used. As an additional safety feature, the whole assembly was contained in a stainless steel blast shield.

Water was added to fill about one third of the chamber from the reservoir. The CO_2 or C_3H_8 gas was then injected into the chamber through valve 1 or 2 from a high-pressure BOC cylinder. The pressurized liquid was then stirred by the spinning flea of the magnetic motor. At sufficiently high pressure and low temperature, the gas hydrate was formed. Fig. 3 shows a formation curve of carbon dioxide hydrate. The volume of gas consumed at a constant pressure of 3.15 MPa during hydrate formation is plotted as a function of time. The initial rise in gas consumption represents the dissolution of gas. This is followed by a plateau (20–40 min) considered to be the nucleation induction period where stable hydrate nuclei are formed. The final rise in gas consumption (above 50 min) occurs as a result of hydrate crystal growth where gas molecules are rapidly enclathrated.

3. Experimental set-up

The above cell was used on the energy-dispersive instrument of station 9.7 at the CCLRC Daresbury Laboratory. With the high-pressure chamber in the 1.0 mm diameter beam, the less energetic photons were heavily absorbed by the cell wall. Diffracted X-rays were detected by an EG&G

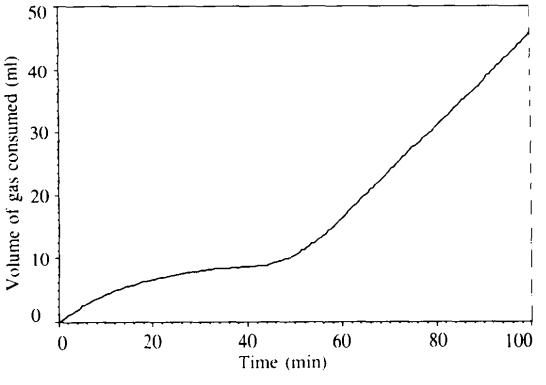

Figure 3
The consumption of CO_2 in the cell as a function of time at T = 273.3 K and P = 3.15 MPa.

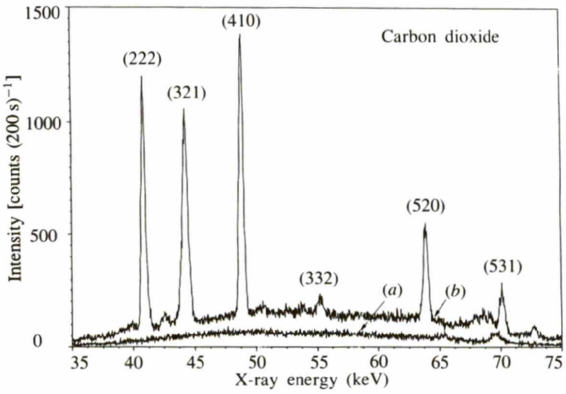

Figure 4
Diffraction spectra of the CO_2 solution (*a*) before crystallization, and (*b*) at crystallization. The raw intensity data are shown. Peaks are indexed with type I structure (see text).

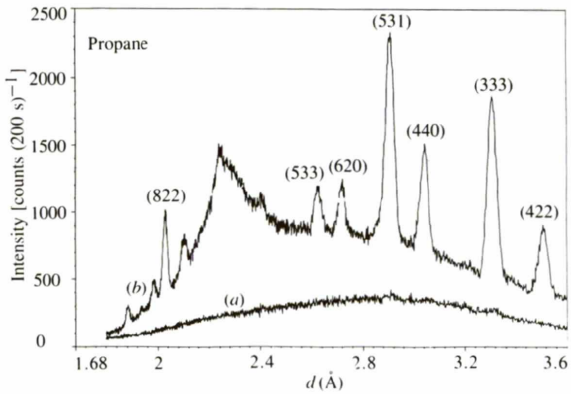

Figure 5
Diffraction spectra of the C_3H_8 solution (*a*) before crystallization, and (*b*) at crystallization. The raw intensity data are shown. Peaks are indexed with type II structure (see text).

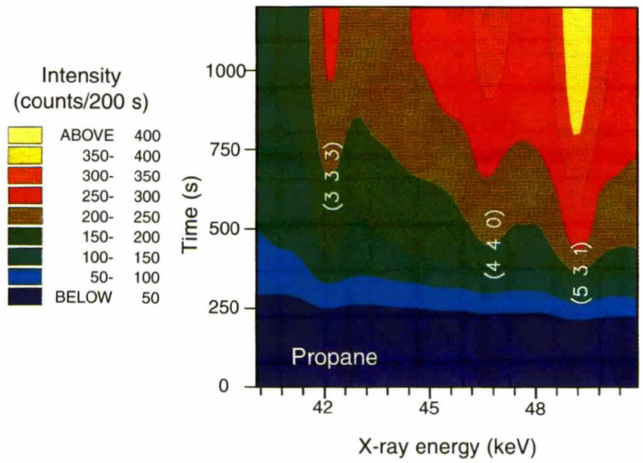

Figure 6
Contour map of the 40–50 keV region showing the formation of the C_3H_8 hydrate. The dominant peaks are the (333), (440) and (531) reflections. Note that the time taken for these peaks to develop fully was *ca* 750 s.

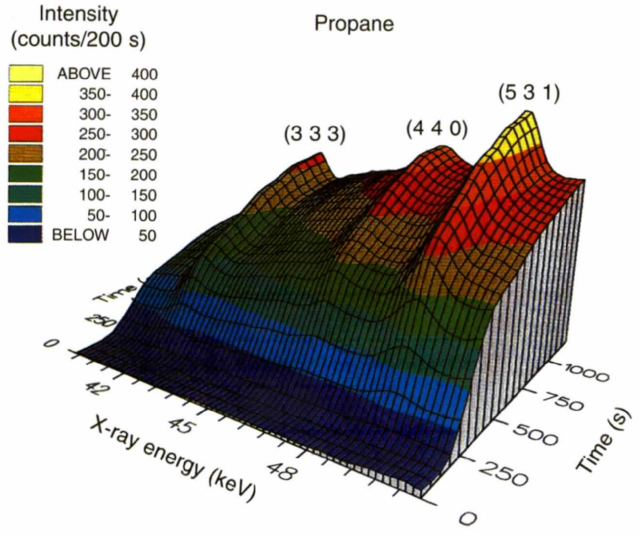

Figure 7
Three-dimensional picture showing the dramatic development of the (333), (440) and (531) reflections. Note that the peaks are on the hydrate hump (light-blue and green regions) above the water background (dark-blue region).

ORTEC germanium solid-state detector with an energy resolution of $\Delta E/E \simeq 0.007$ at 50 keV. A fixed detector angle, 2θ, was defined by a post-sample slit 400 mm long and 10 mm across, with a 0.1 mm gap. The photons were then electronically separated by the instrument multichannel analyzer. Intensity peaks could be obtained as each set of lattice planes of interplanar spacing (d) from the crystalline sample diffracts X-rays of energy given by $E = 6.199/(d \sin\theta)$, where E and d are in keV and Å, respectively. The data-collection software was set up so that a series of intensity-energy spectra could be recorded during the course of material formation. More details of the instrument and data acquisition are given by Clark (1989) and Tang, Miller, Clark, Player & Craib (1996).

4. Results

With the sample cell initially filled with fine NaCl powder, (111), (200), ($\bar{2}$20) and (311) diffraction peaks were measured. Using the fitted peak positions, the 2θ angle was refined to be 5.0402 (5)°. The cell was then loaded with water and carbon dioxide. The mixture was cooled and pressurized to form hydrate crystals and diffraction measurements were made during formation. Fig. 4 presents the spectra collected in a 200 s frame (*a*) before crystallization, and (*b*) at crystallization. The contrast between the two curves is obvious as the appearance of the peaks is clearly attributed to development of the polyhedral clathrate framework. The intensity data on both curves have not been normalized for the transmitted intensity. Using the crystallographic system described previously (structure I), we were able to identify all the peaks on the pattern. Note that only the strong peaks are labelled in the figure. To understand the kinetics of the system, a series of spectra were collected as a function of temperature, pressure or time. The observed reflections were collectively least-squares fitted to Gaussian functions and the determined peak positions were used to refine the cell parameters. These results are summarized in Table 1. A lattice constant of 11.927 (2) Å was obtained at 273.3 K and 3.15 MPa. Apart from the (620) plane, which has the largest error, all the reflections fitted reasonably well. Our cell parameter is slightly lower than the value of 12.07 Å (von Stackelberg & Jahns, 1954). Their value was measured from a single crystal under cryogenic temperatures and atmospheric pressure (*ex situ*) using a conventional X-ray diffraction method.

Similar measurements were carried out on the propane system. The diffraction patterns of a much longer timeframe (30 min) are shown in Fig. 5. Here the energy scale has been converted to interplanar spacing (d) and the intensity data are not normalized. Again we have observed structural peaks during hydrate formation. The indexing of sample peaks is consistent with the expected structure (type II) and only the strong peaks are labelled in the figure. However, there is a large feature centred at approximately 2.35 Å. Although its origin is not clear, this feature coincided with a high propane-clathrate peak density. The contour map (Fig. 6) and three-dimensional picture (Fig. 7) clearly show the formation of the hydrate. In this case, the demonstration is highlighted on the intensity–time dependence of the (333), (440) and (531) reflections. The hydrate crystals started formation at *ca* 250 s and were well developed at 1000 s. Table 2 summarizes the reflections observed and the refined cell parameter for this system at 273.3 K and 0.43 MPa. Again the lattice constant is slightly smaller than the value of 17.40 Å measured by von Stackelberg & Jahns (1954). The kinetics of the structure observed from the two hydrates have been published in detail by Koh, Savidge & Tang (1996).

Table 1
Carbon dioxide hydrate at T = 273.3 K, P = 3.15 MPa.

Refined cell parameter, a = 11.927 (2) Å.

Reflection (hkl)	Peak position (keV) Observed	Calculated	Difference Δ
(222)	40.971 (2)	40.9471	0.0239
(320)	42.593 (3)	42.6191	−0.0261
(321)	44.242 (1)	44.2279	0.0141
(400)	47.318 (8)	47.2816	0.0364
(410)	48.725 (3)	48.7368	−0.0118
(330)	50.141 (3)	50.1497	−0.0087
(421)	54.161 (5)	54.1679	−0.0069
(332)	55.431 (8)	55.4426	−0.0116
(520)	63.632 (7)	63.6548	−0.0228
(530)	68.911 (5)	68.9242	−0.0132
(531)	69.902 (2)	69.9305	−0.0285
(532)	72.803 (5)	72.8659	−0.0629
(620)	74.91 (1)	74.7588	0.1512

Table 2
Propane hydrate at T = 273.3 K, P = 0.43 MPa.

Refined cell parameter, a = 17.196 (2) Å.

Reflection (hkl)	Peak position (keV) Observed	Calculated	Difference Δ
(422)	40.173 (4)	40.1656	0.0074
(333)	42.616 (2)	42.6020	0.0140
(440)	46.365 (4)	46.3792	−0.0142
(531)	48.511 (3)	48.5045	0.0065
(620)	51.857 (6)	51.8535	0.0035
(533)	53.713 (7)	53.7629	−0.0499
(733)	67.08 (1)	67.1098	−0.0298
(822)	69.496 (3)	69.5688	−0.0728
(555)	71.01 (1)	71.0034	0.0066

5. Conclusions

The overall diffraction results presented in Tables 1 and 2 for CO_2 (structure I) and C_3H_8 (structure II) hydrates, respectively, are consistent with previous studies. The results have demonstrated the feasibility of the technique for collecting *in-situ* lattice information during gas hydrate crystallization. It has the potential for obtaining integrated intensity for more detailed structural information in future studies. The new technique has been applied to the study of a range of crystallization variables on hydrate formation (Koh, Savidge & Tang, 1996).

The financial support of the Gas Research Institute, Chicago, IL, USA, is gratefully acknowledged. The authors are grateful to Mr J. Flaherty (Daresbury) for his assistance in the design of the cell, and Mr A. C. Jupe (Birkbeck) for his help in some of the measurements. We would like to thank EPSRC for provision of beam time.

References

Clark, S. M. (1989). *Nucl. Instrum. Methods*, **A276**, 381–387.

Davidson, D. W. (1973). *Water – a Comprehensive Treatise*, Vol. 2, edited by F. Frank, pp. 115–234. New York/London: Plenum Press.

He, H., Barnes, P., Munn, J., Turrillas, X. & Klinowski, J. (1992). *Chem. Phys. Lett.* **196**, 267–273.

Jeffrey, G. A. (1984). *Inclusion Compounds*, Vol. 1, pp. 135–190. London: Academic Press.

Jeffrey, G. A. & McMullan, R. K. (1967). *Prog. Inorg. Chem.* **8**, 43–108.

Koh, C. A., Savidge, J. L. & Tang, C. C. (1996). *J. Phys. Chem.* **100**, 6412–6414.

Kuhs, W. F., Dorwarth, R., Londono, J. D. & Finney, J. L. (1992). *Physics and Chemistry of Ice*, edited by N. Maeno & T. Hondoh, pp. 126–130. Sapporo: Hokkaido University Press.

Savidge, J. L., Koh, C. A., Motie, R. E., Nooney, R. I. & Wu, X. (1996). *Proc. Int. Gas Res. Conf.*, Cannes, France, November 1995. In the press.

Sloan, E. D. Jr (1992). *The State-of-the-Art of Hydrates as Related to the Natural Gas Industry*. Topical Report GRI-91/0302, June 1992. Gas Research Institute, Chicago, IL, USA.

Stackelberg, M. von & Jahns, W. (1954). *Z. Elektrochem.* **58**, 162–164.

Tang, C. C., Miller, M. C., Clark, S. M., Player, M. A. & Craib, G. R. G. (1996). *J. Synchrotron Rad.* **3**, 6–13.